FILTERED-X NLMS ALGORITHM WITH COMPENSATION OF MEMORYLESS NONLINEARITIES FOR ACTIVE NOISE CONTROL

Giovanni L. Sicuranza and Alberto Carini

DEEI, University of Trieste
Via A. Valerio 10, 34127, Trieste, Italy
phone: + (39) 558 3452, fax: + (39) 558 3460
email: sicuranza@univ.trieste.it
web: www.units.it/ ipl/

STI, University of Urbino
Piazza della Repubblica 13, 61029, Urbino, Italy
phone: + (39) 0722 447548, fax: + (39) 0722 447552
email: carini@sti.uniurb.it
web: www.sti.uniurb.it/carini/

ABSTRACT

In this paper we consider the problem of deriving an efficient adaptation algorithm when the secondary path of a single-channel feed-forward Active Noise Control (ANC) system contains a memoryless nonlinearity affecting the output of the controller. In order to avoid complex nonlinear adaptation strategies, the solution proposed consists in the design of a predistorter that linearizes the input-output relationship of the memoryless nonlinearity. The linearization technique exploits the histograms and the cumulative density functions of the input and output signals. Then, we show how the linear NLMS adaptation algorithm can be suitably modified and applied in the framework of a feed-forward delay-compensated scheme. Theoretical considerations are developed to show that the algorithm is in general affected by a bias that depends on the deviations of the linearized model from the ideal linear input-output characteristic. The results of the reported experiments confirm, in agreement with the theoretical analysis, that the accurate design of the predistorter can reduce the bias so that useful results can be obtained.

1. INTRODUCTION

Active noise control (ANC) is based on the destructive interference in a given location of the noise produced by a primary noise with a secondary signal, having the same amplitude and opposite phase. The interfering signal is generated by a suitable actuator driven by an adaptive controller, and propagated through the so-called secondary path up to the canceling zone [1]. In the feed-forward schemes, the controller is usually implemented as an FIR filter and updated by means of Filtered-*x* versions of the standard adaptive algorithms. The input signal, sensed by the reference microphone located in proximity of the noise source, and the signal gathered by the error microphone located at the canceling zone are used to this purpose. While the literature is mainly concerned with linear controllers, it is well known that nonlinearities may influence the behavior of an ANC system. In fact, in actual systems the source noise may be modeled as a nonlinear process, the primary path may exhibit some nonlinear behavior, and the secondary path may be also affected by nonlinear distortions. Among all nonlinear effects, the most common distortions are those affecting the secondary path, since they are mainly due to saturation of the electronic components, such as microphones, analog-to-digital converters, preamplifiers, power amplifiers and loudspeakers, exploited to generate the interfering signal. It is worth noting that while linear components are usually quite expensive, the use of low-cost devices in the controller permits the realization of ANC systems with reduced costs but at the expense of noticeable nonlinearities. On the other hand, the most difficult situation to deal with is when the nonlinearities affect the secondary path. In fact, in this case the optimal solution of the ANC problem requires the derivation of an exact, or at least an approximate, inverse of a nonlinear relationship. As a consequence, this operation is usually computationally intensive. Moreover, the MSE cost function is no more, in general, quadratic and thus the adaptive algorithms may converge to local minima.

As a matter of fact, a nonlinear system for ANC can be divided in two categories, depending on the linearity or nonlinearity, respectively, of the secondary path. With reference to the first class of ANC systems, various nonlinear controllers have been proposed in the literature using, in general, adaptive polynomial filters or artificial neural networks exploiting functional expansions [2] - [6]. In contrast, few solutions have been proposed to specifically deal with nonlinear effects in the secondary path. Moreover, most of them are limited to the application of fixed controllers, designed using multilayer artificial neural networks [7], [8] and optimizations based on genetic algorithms [9]. Recently, an accurate study of a class of nonlinear controllers based on functional expansions in presence of nonlinearities in the secondary path has been performed in [10]. Nonlinear adjoint LMS-based algorithms, that can reduce to some extent the computational complexity with respect to the corresponding nonlinear Filtered-*x* LMS-based algorithms, have been presented. Specific solutions can be also found in the literature, dealing with the problems of signal saturation and other nonlinear distortions that occur in ANC systems used for practical applications, such as the saturation effects on the input signal at the reference microphone [11] or at the output of the actuator [12]. In [11] bilinear filters are used to take into account the memory effects introduced by the impulsive response of the the secondary path. In [12] the attention is centered on the nonlinearity affecting the power amplifier and/or the loudspeaker at the output of the controller, modeled as a memoryless function while the transfer function of the secondary path is assumed equal to one. The proposal is to use a linear controller equipped with a linear LMS algorithm with leakage. This approach avoids the complexity of a nonlinear LMS algorithm and the identification of the system nonlinearity. However, the model studied in [12] is not directly applicable to a general ANC system.

The method we present in this paper preserves the idea of resorting to a linear algorithm even in presence of a memoryless nonlinearity localized at the output of the controller in the secondary path. Our proposal is to linearize such a nonlinearity using the histogram-based compensation described in [13]. Then, a suitably modified linear NLMS algorithm can be applied. We also show that this modified NLMS algorithm is in general affected by a bias that depends on the deviations of the linearized model from the ideal linear input-output characteristic. Nevertheless, the accurate design of the predistorter can reduce the bias so that useful results can be obtained, as shown in the reported experiments.

The paper is organized as follows. In Section 2, the histogram-based identification and compensation of a memoryless nonlinear device is briefly reviewed. Then, the linear Filtered-x NLMS algorithm is suitably modified to include such a compensation technique in the scheme with delay compensation of a single-channel feed-forward ANC system. The derived algorithm is analyzed in Section 3, where its theoretical properties are investigated. The results of computer simulations are reported in Section 4. The conclusions follow in Section 5.

2. THE FILTERED-X NLMS ALGORITHM WITH NONLINEARITY COMPENSATION

We refer in this Section to a single-channel feed-forward ANC structure, equipped with the Filtered-x NLMS algorithm, and including a memoryless nonlinearity in the secondary path at the output of the controller. While nonlinearities with memory usually happen in high-quality audio equipments [14], memoryless nonlinearities occur typically at low-cost power amplifiers or loudspeakers. Since our aim is to design a low-cost ANC system, we limit in this paper our attention to memoryless nonlinearities representing the distortions due to the power amplifier and/or the loudspeaker at the output of the controller. It is worth noting that, in presence of other nonlinearities affecting the noise source or the primary path, it is possible to extend the modified linear NLMS algorithm described below to nonlinear controllers as those based on the class of filters in which the output depends linearly on the filter coefficients [6]. In our experimental set-up we consider two phases of operation of the ANC system. In the first phase (modeling or learning phase), we characterize the nonlinear device measuring the signals at the input and at the output of the power amplifier or the loudspeaker. To this purpose, the histogram-based method described in [13] is applied. While in principle any kind of signal filling all the bins of the histogram can be profitably applied, it can be convenient to directly use the the samples incoming from the noise source. Then, in the second phase (adaptation or noise-controlling phase), we operate the ANC system by adapting the control filter and we keep fixed the linearized model of the nonlinearity.

2.1 The histogram-based compensation

Let us first summarize the histogram-based technique for the compensation of a memoryless nonlinearity. The theoretical foundations and further details can be found in [13]. Our aim is to design a predistorter PD, placed before a memoryless nonlinear device NL, so that the output $y(n)$ is a linearized replica copying the input signal $r(n)$, as schematically shown in Figure 1. During the modeling (or learning) phase, the signal $r(n)$ coincides with the primary noise source $x(n)$. We assume that the input and output signals of the nonlinear device NL are included in the intervals $-X \div X$ and $-Y \div Y$, respectively, with $X = \max_n |x(n)|$ and $Y = \max_n |y(n)|$. The method requires the evaluation of the histograms of these signals, normalized between 0 and 1, on a given number N of bins. Then, the corresponding cumulative density functions, $P_r(r(n))$ and $P_y(y(n))$ can be computed as the sums, normalized between 0 and 1, of all the respective values of the present and preceding histogram bins. During the adaptation phase, the linearization of the memoryless nonlinearity is achieved if the output from the predistorter PD in Figure 1 (b) satisfies the relation $P_y(r(n)) = P_r(u(n))$. In other words, the output $u(n)$ from the predistorter that linearizes the output from the nonlinear device NL can be computed as $u(n) = P_r^{-1}(P_y(r(n))$ [13]. Since P_y and P_r are discrete functions, defined only for the values marking the histogram bins, two interpolations are required to compute the actual value of $P_y(r(n))$ and then of $u(n)$ on the continuous interval $0-1$. Both the direct and inverse calculations are usually performed connecting with a linear segment the adjacent points of P_y and P_r, respectively. Thus the block PD shown in Figure 1 (b) has an input-output relationship defined by these two linear interpolations. It is worth noting that the accuracy of the histogram-based model of the nonlinearity, derived during the learning phase, depends on the deviations between the ideal linear relationship and the actual result of the linearization procedure. Therefore, for small values of the number of bins, there are possibly large errors due to the small number of points supporting the interpolations of P_y and P_r. On the other side, for large values of N, there are possibly large errors due to the fact that not all the bins of the histograms are visited during the learning phase. As a consequence, the two curves P_r and P_y are no more strictly monotonically increasing, as required from the theory in [13], and inconsistencies may appear in the evaluation of the output from the predistorter. Such considerations motivate the choice on an appropriate intermediate value for N, and also the use of some simple preprocessing in order to profitably exploit the input signal in the initial learning phase, as shown in Section 4.

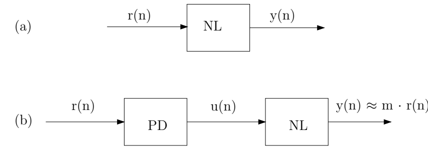

Figure 1: (a) Memoryless nonlinearity NL, (b) compensation of NL with a predistorter PD.

2.2 The modified Filtered-x NLMS algorithm

Throughout the paper, a feed-forward delay-compensated scheme [15] is adopted to compensate for the propagation delay introduced by the secondary path. This scheme is modified as shown in Figure 2 to include the linearization of a memoryless nonlinear device in the secondary path. The output $d(n)$ of the physical primary path $P(z)$ is estimated as $\hat{d}(n)$ by adding the output $\hat{y}'(n)$ of the model $\hat{S}(z)$ of the physical secondary path $S(z)$ to the error sensor signal $e(n) = d(n) - y'(n)$. The error $g(n)$ is then used to update the weights of $W(z)$ and these weights are finally copied to the controller. While preliminary and independent evalua-

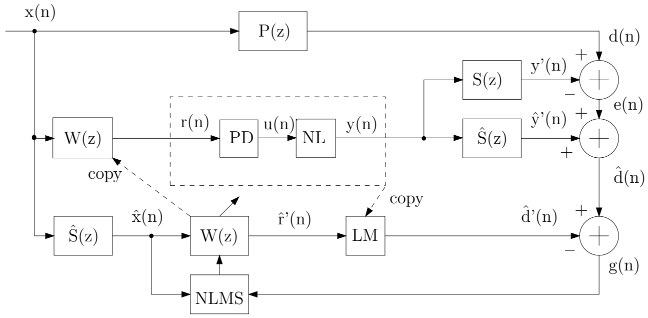

Figure 2: Block diagram of delay-compensated feed-forward Filtered-x structure with nonlinearity compensation.

tion of the transfer function of the secondary path is needed, the nonlinear device is modeled during the learning phase, as described in Subsection 2.1. During the adaptation phase, the histogram-based compensation is used, as indicated in the dashed box. The linearized input-output relationship of the predistorter cascaded with the nonlinear device should be included in the adaptation loop (the block LM in Figure 2). The block LM is simply modeled by a linear gain depending on the range of the input and output signals of NL. This elementary model is preferred to more accurate representations, as for example the linear regression line that, in contrast, is more computationally expensive and may include a constant term (an offset) that negatively affects the residual errors. The filter output in the controller is given by the equation (1)

$$r(n) = \mathbf{x}^T(n)\mathbf{w}(n), \tag{1}$$

where $\mathbf{w}(n)$ is the vector formed with the M coefficients of the control FIR filter

$$\mathbf{w}(n) = [w(n,0), w(n,1), \ldots, w(n,M-1)]^T, \tag{2}$$

and $\mathbf{x}$ is the vector formed with the last M samples of the primary noise signal

$$\mathbf{x}(n) = [x(n), x(n-1), \ldots, x(n-M+1)]^T. \tag{3}$$

The signal $r(n)$ is used, together with the auxiliary signal $u(n)$, derived as described in Subection 2.1, to obtain the linearized output $y(n)$. With reference to Figure 2 we can also derive the following expressions. The output of the physical secondary path $y'(n)$ is given by

$$y'(n) = s(n) * y(n), \tag{4}$$

where the symbol $*$ indicates the linear convolution and $s(n)$ is the finite impulse response of the physical secondary path $S(z)$. Similarly, the output of the model of the secondary path $\hat{y}'(n)$ is given by

$$\hat{y}'(n) = \hat{s}(n) * y(n), \tag{5}$$

where $\hat{s}(n)$ is the impulse response of the model $\hat{S}(z)$ of the secondary path $S(z)$. The input signal $x(n)$ is filtered by the finite impulse response $\hat{s}(n)$ to obtain the signal $\hat{x}(n)$ at the input of the adaptation loop

$$\hat{x}(n) = \hat{s}(n) * x(n). \tag{6}$$

Then it results

$$\hat{r}'(n) = \hat{\mathbf{x}}^T(n)\mathbf{w}(n), \tag{7}$$

where $\hat{\mathbf{x}}(n)$ is the vector formed with the the last M samples of the filtered input signal

$$\hat{\mathbf{x}}(n) = [\hat{x}(n), \hat{x}(n-1), \ldots, \hat{x}(n-M+1)]^T. \tag{8}$$

The output $\hat{d}'(n)$ from the block LM is computed as

$$\hat{d}'(n) = m \cdot \hat{r}'(n), \tag{9}$$

where $m = Y/X$ is the gain parameter of the ideal linear model of the predistorter cascaded with the nonlinear device NL. Then,

$$e(n) = d(n) - y'(n) \tag{10}$$

is the error to be minimized at the location where it is placed the error microphone, and

$$g(n) = \hat{d}(n) - \hat{d}'(n) \tag{11}$$

is the error used to update the filter coefficients together with the filtered input signal, where

$$\hat{d}(n) = e(n) + \hat{y}'(n). \tag{12}$$

By minimizing the MSE of $g(n)$, according to the NLMS algorithm, the following updating equation for the filter coefficients is derived

$$\mathbf{w}(n+1) = \mathbf{w}(n) + \mu g(n)\hat{\mathbf{x}}(n)/(\hat{\mathbf{x}}^T(n)\hat{\mathbf{x}}(n) + \delta), \tag{13}$$

where μ is the adaptation step-size and δ is a small constant value used to avoid possible singularities of the correlation matrix $\hat{\mathbf{x}}^T(n)\hat{\mathbf{x}}(n)$.

The computational costs of the whole procedure include the operations required in the learning phase and in the successive adaptation phase. During the learning phase, the calculations of two histograms and two cumulative density functions are required. The corresponding number of operations depends on the number of samples used during the learning phase and the number of histogram bins. As shown by our experiments, both these values can be suitably limited. Then, in the working ANC phase, the operations per sample required are those of the standard linear NLMS algorithm plus one multiplication for the application of the linearized model in the adaptation loop and four multiplications and four additions for the direct and inverse interpolations in the predistorter. Therefore, the total complexity is only a little higher than that of a linear controller.

3. ANALYSIS OF THE MODIFIED FILTERED-X NLMS ALGORITHM

We first consider the minimum mean square (MMS) solution of the ANC problem of Figure 2 in the most general case when the cascade of the predistorter PD and of the nonlinearity NL is equivalent to a memoryless nonlinear system: $y(n) = f(r(n))$. It is assumed that the function $f(x)$ can be expanded in the Taylor series:

$$f(x) = f(0) + f'(0)x + \frac{1}{2!}f''(0)x^2 + \ldots. \tag{14}$$

with f' the first derivative of f, f'' the second derivative of f, etc.

According to the hypothesis that the matrix $E\Big\{\big\{s(n) * \big[f'(\mathbf{w}_o^T\mathbf{x}(n))\mathbf{x}(n)\big]\big\}\cdot \big\{s(n) * \big[f'(0)\mathbf{x}(n)\big]\big\}^T\Big\}$ is invertible, the MMS solution of the active noise control problem $\mathbf{w}_o$,

$$\mathbf{w}_o = \min_{\mathbf{w}}\big\{E\{e^2(n)\}\big\} = = \min_{\mathbf{w}}\Big\{E\big\{\big[d(n) - s(n) * f(\mathbf{w}^T\mathbf{x}(n))\big]^2\big\}\Big\}, \tag{15}$$

is given by the fixed point of the following equation:

$$\mathbf{w}_o = E\Big\{\big\{s(n) * \big[f'(\mathbf{w}_o^T\mathbf{x}(n))\mathbf{x}(n)\big]\big\} \cdot\big\{s(n) * \big[f'(0)\mathbf{x}(n)\big]\big\}^T\Big\}^{-1} \cdot E\Big\{\big[d(n) - s(n) * f(0)\big]\cdot\big\{s(n) * \big[f'(\mathbf{w}_o^T\mathbf{x}(n))\mathbf{x}(n)\big]\big\} - \frac{1}{2}\big[f''(0)s(n) * (\mathbf{w}_o^T\mathbf{x}(n))^2\big] \cdot\big\{s(n) * \big[f'(\mathbf{w}_o^T\mathbf{x}(n))\mathbf{x}(n)\big]\big\} + \ldots\Big\}. \tag{16}$$

Indeed, by setting to zero the derivative of the term $E\Big\{\big[d(n) - s(n) * f(\mathbf{w}^T\mathbf{x}(n))\big]^2\Big\}$ with respect to $\mathbf{w}$, and replacing $\mathbf{w}$ with $\mathbf{w}_o$, we get:

$$-2E\Big\{\big[d(n) - s(n) * f(\mathbf{w}_o^T\mathbf{x}(n))\big] \cdot\big\{s(n) * \big[f'(\mathbf{w}_o^T\mathbf{x}(n))\mathbf{x}(n)\big]\big\}\Big\} = 0. \tag{17}$$

Moreover, by replacing $f(\mathbf{w}_o^T\mathbf{x}(n))$ with its Taylor series expansion and by manipulating the resulting equation, we obtain the result of Equation (16).

In the hypothesis that $f(x)$ is a linear function, i.e. $f(x) = m\cdot x$, we obtain the following closed expression for $\mathbf{w}_o$:

$$\mathbf{w}_o = \frac{1}{m}E\big\{\mathbf{x}'(n)\mathbf{x}'^T(n)\big\}^{-1}\cdot E\big\{d(n)\mathbf{x}'(n)\big\}, \tag{18}$$

where $\mathbf{x}'(n) = s(n) * \mathbf{x}(n)$. Moreover, in the hypothesis that the nonlinear system has mild nonlinearities, i.e., in the hypothesis that $f(0) + f'(0)x \gg \frac{1}{2}f''(0)x^2 + \ldots$ and $f(x) \simeq f(0) + f'(0)x \simeq m\cdot x$ in the range of interest of x, the expression of Equation (18) provides an approximate estimate of the MMS solution given by Equation (16).

Let us now consider the adaptation equation of (13), with

$$g(n) = \hat{d}(n) - m\cdot\mathbf{w}^T(n)\hat{\mathbf{x}}(n) \tag{19}$$

regardless $f(x)$ being a linear or a nonlinear function. If we replace (19) in (13), we take the expectation of the two members, and we consider the fixed point of the resulting equation, in the hypothesis of a perfect modeling of the secondary path (i.e., $\hat{s}(n) = s(n)$, $\hat{d}(n) = d(n)$, and $\hat{\mathbf{x}}(n) = \mathbf{x}'(n)$) and of (13) being convergent, it is proven that $\mathbf{w}(n)$ tends to the coefficient vector in (18). Thus, in case $f(x) = m\cdot x$, the algorithm converges to the MMS solution of the ANC problem. On the contrary, if $f(x) \neq m\cdot x$, even in the hypothesis of mild nonlinearities Equation (18) provides only an approximate estimate of (16) and the adaptation in (13) converges to a biased solution for the ANC problem. Nevertheless, the smallest is the deviation of $f(\cdot)$ from the ideal linear characteristic, the smallest is the bias in the estimation of the coefficient vector in (16).

Eventually, it should be noted that in the hypothesis of a perfect modeling of the secondary path the adaptation rule in (13) can also be written as

$$\mathbf{w}(n+1) = \mathbf{w}(n) + (\mu m)\cdot\hat{g}(n)\hat{\mathbf{x}}(n)/(\hat{\mathbf{x}}^T(n)\hat{\mathbf{x}}(n) + \delta), \tag{20}$$

with

$$\hat{g}(n) = \frac{d(n)}{m} - \mathbf{w}^T(n)\hat{\mathbf{x}}(n). \tag{21}$$

Equation (20) coincides with the adaptation equation of the NLMS algorithm with step-size μm, input signal $\hat{x}(n)$ and desired signal $d(n)/m$. Thus, the adaptation equation in (13) has the same convergence properties (e.g., convergence speed, mean square error, mean square deviation) of this NLMS algorithm and, in particular, it is convergent when $0 < \mu < 2/m$.

4. EXPERIMENTAL RESULTS

We consider a multitonal signal composed of three sinusoids at frequencies 160, 320 and 640 Hz sampled at the sampling frequency of 8000 Hz. The input signal is normalized to a unit power and a Gaussian noise with 30 dB of attenuation is added. All the reported data are averaged on 100 independent tests using a different seed for the Gaussian noise and random phases for the three sinusoids. The memoryless nonlinear device is represented by the input-output relation

$$y(n) = A\cdot\tanh(b\cdot x(n))/b, \tag{22}$$

that well represents the saturation behavior of a power amplifier. In the tests, it has been fixed $A = 3$ and $b = 1.8$. The primary and secondary paths have been obtained by truncating to 93 samples the impulse responses of the acoustic paths reported in the companion disk of [1]. For simplicity's sake, the perfect modeling condition is assumed in the example, i.e. $\hat{S}(z) = S(z)$. The output of the primary path has been corrupted with a white Gaussian noise with a 40 dB signal to noise ratio. The controller is an FIR filter with 32 taps. The adaptation parameters have been chosen as $\mu = 0.01$ and $\delta = 0.001$. Table 1 shows the residual power at the microphone error, i.e. an estimation of $E[e^2(n)]$, and the Mean-Square Deviation between the linearized model and the ideal linear characteristic as a function of the histogram bins. The columns with $L = 1$ refer to the direct use of 1000 samples of the multitonal noise during the learning phase. Due to the approximation errors in the linearization of the nonlinear characteristic, there is a bias affecting this situation, as shown in Section 3. From the analysis of the used data, it appears that the reason is mainly due to the errors arising because there are empty bins in the histograms. A simple remedy to this fact consists of using during the learning phase an interpolation with a factor $L = 3$ on the input and output signals of the nonlinear device. In practice, in this case, the used 3000 samples are distributed so that there are no more empty bins and thus the linearization is affected by reduced errors. The last line in Table 1 indicates the residual power for the ANC system without the nonlinear block NL, adapted with

Number of bins	Residual Power		MS Deviation	
	L=1	L=3	L=1	L=3
21	0.0970	0.0629	0.0447	0.0360
41	0.0563	0.0251	0.0154	0.0094
61	0.0448	0.0178	0.0094	0.0044
81	0.0661	0.0157	0.0123	0.0027
101	0.0588	0.0148	0.0095	0.0017
Linear case	0.0100		0.0000	

Table 1: Residual power and Mean-Square Deviation from linearity.

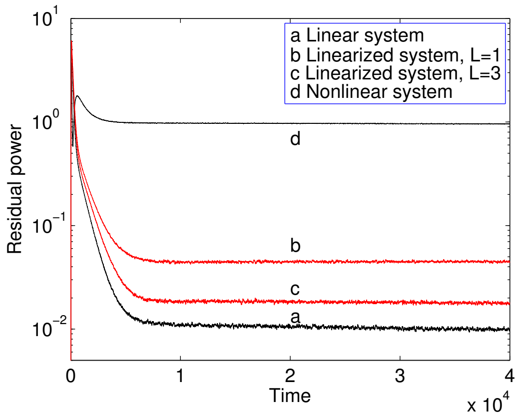

Figure 3: Adaptation curves.

the standard linear NLMS algorithm. This residual power can be considered as the unbiased limit to which tends the modified NLMS algorithm in presence of the nonlinear block NL. Even though better results are steadily obtained by increasing the number of bins with $L = 3$, a computationally efficient compromise can be obtained for 61 bins. Figure 3 shows the ensemble adaptation curves, where each point is evaluated as the mean value over 50 successive samples, representing the residual power measured at the microphone error for: (a) the ANC system without the nonlinear block NL, adapted with the standard linear NLMS algorithm, (b) the ANC system with the nonlinear block NL and without interpolation ($L = 1$), adapted with the modified NLMS algorithm (61 bins), (c) the ANC system with the nonlinear block NL and with interpolation ($L = 3$), adapted with the modified NLMS algorithm (61 bins), and (d) the ANC system with the nonlinear block NL, adapted with the standard linear NLMS algorithm. The curve (c) clearly shows the reduction of the bias with respect to the curve (b), according to the theoretical considerations and the data in Table 1.

5. CONCLUDING REMARKS

In this paper it has been shown how the histogram-based compensation of a memoryless nonlinearity can effectively work also in the case of a feed-forward ANC system including this kind of nonlinearity in the secondary path. The modified linear NLMS adaptation algorithm proposed in this paper is simple and efficient. A theoretical analysis of the behavior of the method, with particular reference to the influence of the errors that affect the histogram-based linearization, is presented to confirm the validity of the proposed approach. It is worth stressing the fact that this approach allows the design of efficient ANC systems using low-cost devices in the controller in spite of their nonlinear characteristics.

REFERENCES

[1] S. M. Kuo and D. R. Morgan, *Active noise control Systems – Algorithms and DSP implementation*. New York: Wiley, 1996.

[2] P. Strauch and B. Mulgrew, “Active control of nonlinear noise processes in a linear duct,” *IEEE Trans. Signal Processing*, vol. 46, pp. 2404–2412, Sept. 1998.

[3] L. Tan and J. Jiang, “Adaptive Volterra filters for active noise control of nonlinear processes,” *IEEE Trans. Signal Processing*, vol. 49, pp. 1667-1676, Aug. 2001.

[4] G. L. Sicuranza and A. Carini, “Filtered-X Affine Projection algorithm for multichannel active noise control using second-order Volterra filters,” *IEEE Signal Processing Letters*, vol. 11, pp. 853-857, Nov. 2004.

[5] D. P. Das and G. Panda, “Active mitigation of nonlinear noise processes using a novel filtered-s lms algorithm,” *IEEE Trans. Speech and Audio Processing*, vol. 12, pp. 313–322, May 2004.

[6] A. Carini and G. L. Sicuranza, “Transient and steady-state analysis of Filtered-X Affine Projection algorithms,” *IEEE Trans. Signal Processing*, vol. 54, pp. 665-678, February 2006.

[7] S. D. Snyder and N. Tanaka, “Active control of vibration using a neural network,” *IEEE Trans. Neural Networks*, vol. 6, pp. 819-828, July 1995.

[8] M. Bouchard, B. Paillard and C. T. L. Dinh, “Improved training of neural networks for the nonlinear active noise control of sound and vibration,” *IEEE Trans. Neural Networks*, vol. 10, pp. 391-401, March 1999.

[9] F. Russo and G. L. Sicuranza, “Accuracy and Performance Evaluation in the Genetic Optimization of Nonlinear Systems for Active Noise Control, ” *IEEE Trans. Instrum. Measur.*, vol. 56, pp. 1443-1450, August 2007.

[10] D. Zhou and V. DeBrunner, “Efficient adaptive nonlinear filters for nonlinear active noise control,” *IEEE Trans. Circuits Syst. I*, vol. 54, pp. 669-681, March 2007.

[11] S. M. Kuo and H. T Wu, “Nonlinear adaptive bilinear filters for active noise control systems,” *IEEE Trans. Circuits Syst. I*, vol. 52, pp. 617-624, March 2005.

[12] O. J. Tobias and R. Seara, “On the LMS algorithm with constant and variable leakage factor in a nonlinear environment,” *IEEE Trans. Signal Processing*, vol. 54, pp. 3448-3458, Sep. 2006.

[13] D. Huang, X. Huang and H. Leung, “Nonlinear compensation of high-power amplifier distortion for communication using a histogram-based method,” *IEEE Trans. Signal Processing*, vol. 54, pp. 4343-4351, Nov. 2006.

[14] F. X. Y. Gao and W. M. Snelgrove, “Adaptive linearization of a loudspeaker,” *Proc. IEEE ICASSP*, pp. 3589-3592, Toronto, Canada, May 1991.

[15] E. Bjarnason, “Active noise cancellation using a modified form of the filtered-X LMS algorithm,” Proc. EUSIPCO-92, Signal Processing VI, Brussels, Belgium, vol. 2, pp. 1053-1056, Aug. 1992.